Int J Adv Manuf Technol (2015) 77:1315–1331
DOI 10.1007/s00170-014-6544-6

ORIGINAL ARTICLE

# Investigations on relations between shape defects and thickness profile variations in thin flat rolling

**Babak Moazeni · Mahmoud Salimi**

Received: 4 July 2012 / Accepted: 24 October 2014 / Published online: 9 November 2014


**Abstract** In rolling of wide strip, longitudinal compressive stresses develop as a result of nonuniform deformation along the plate width, which enhance long-shape wave. Theoretical assessment of these stresses and factors affecting their magnitude and distributions are not emphasized in existing solutions, since most of the solutions are based on the assumption of plane strain along the entire width. In present investigation, a 3D model of cold rolling process of steel is simulated using the finite element method (FEM) to analyze the flow of material and stresses developed in steady-state wide strip cold rolling of plate with nonuniform thickness profile. The results show that the transition from a flat state to bad shape for specific ratio of output thickness to the width of plate occurs as a result of thickness profile changes, and it is also shown that the critical crown ratio changes in edge wave development are smaller than the middle one.

**Keywords** Flat rolling · Thickness profile · Shape defects · Residual stress · Finite element method

**List of Symbols**

| | |
|---|---|
| $h_b$,$h_j$ | Initial thickness |
| $h_f$,$h_p$ | Final thickness |
| $C_j$ | Initial crown |
| $C_p$ | Final crown |
| $b$ | Plate width |
| $\overline{\sigma}$ | Flow stress |
| $k$ | Material coefficient |
| $\overline{\varepsilon}$ | Equivalent strain |

B. Moazeni (✉) · M. Salimi
Mechanical Engineering Department, Isfahan University of Technology, Isfahan 84156-83111, Iran
e-mail: moazeni.babak@gmail.com

M. Salimi
e-mail: salimi@cc.iut.ac.ir

## 1 Introduction

Strong competition in industry requires the metal forming technologist to strive for high level of quality products. The specification requirements with respect to the flatness of strip are more rigorous than ever before. In steel industry, much attention has been devoted to investigation on flatness of cold-rolled strip due to gradually but continuously increasing demand for improved properties and quality of the final product. Loss of flatness is becoming an increasingly prominent problem as the demand for cold-rolled strip to thinner gauges increases and quality requirements of the market increase, to maintain international competitiveness.

In recent years, a great deal of attention has been paid to the shape defects that take place in rolling, whether it is related to nonuniformity of the roll gap or the initial cross-sectional geometry of strip. Hence, many techniques have been developed to enable higher-quality product in terms of flatness and thickness profile [1].

During the rolling process of thin flat products, i.e., long metal strips, the development of residual stresses, acting predominantly in the longitudinal direction (rolling direction) of strip, is inevitable. They are originated by even very small differences in the opening of the roll gap along the width of the plate leading to small variations in the thickness reduction and as a consequence of the incompressibility of plastic deformations, to longitudinal stresses.

Since the plates are assumed to be thin, they are prone to buckle even under small compressive membrane forces. Hence, it happens frequently that during the release of the global tensile force, buckling and postbuckling can be observed leading to different form of wavy plates. If the residual stresses are small (within the strength of material to buckling), the plate remains flat as shown in Fig. 1a. If the residual stresses are large in comparison to the plate strength, wavy edges or center buckle would emerge. Edge wave occurs if the

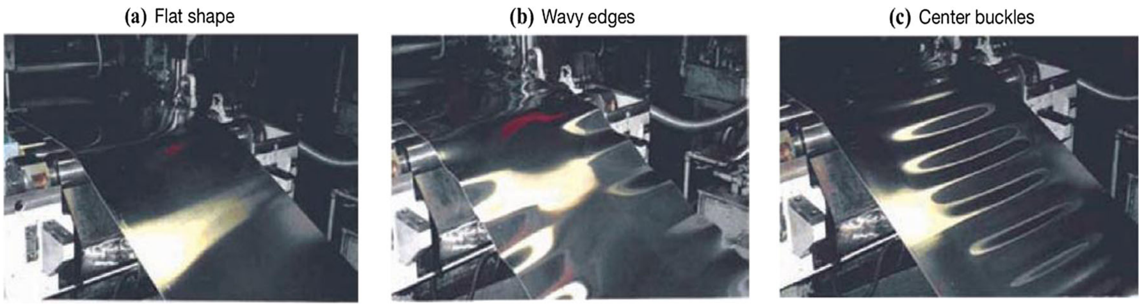


**Fig. 1** Shape defects [2]

edges are under compression (or the center is under tension) as shown in Fig. 1b. If the center is under compression (or the edge is under tension), the result would be the center buckle defect (Fig. 1c).

The problem of excessive residual stress in cold-rolled flat products represents an important source of production loss. Its importance is evident from the number of papers that address this issue, colloquially termed "shape". The initial physical-based models for the prediction of residual stress were developed nearly 40 years ago with the work of Wistreich [3], Shohet and Townsend [4], and Sabatini and Yeomans [5]. The mechanism proposed for the production of residual stress was that it was caused by a variation in the reduction that occurs in the transverse direction of the strip, and hence, it may be calculated as simply the product of the strain variation and the modulus of elasticity of the strip.

Classical literature dealing with strip flatness can be found in research by Tarnopolskaya [6]. Further investigations of buckling during rolling of sheet metal are presented in the study of Komori [7]. More recently, some papers [8–11] have dealt with these kinds of instabilities by analytical considerations (based on a Ritz approach in conjunction with variational methods) as well as computational investigations (in the form of nonlinear finite element analysis).

In order to investigate the effective parameters on nonuniform deformation of strip, Townsend and Shohet [12] and Hu et al. [13] studied the effect of thickness profile variations on shape of the strip. In addition, Malik and Grandhi [14] develop

**Fig. 2** Schematic diagram of principal types of buckling and the stress distributions probably associated with them

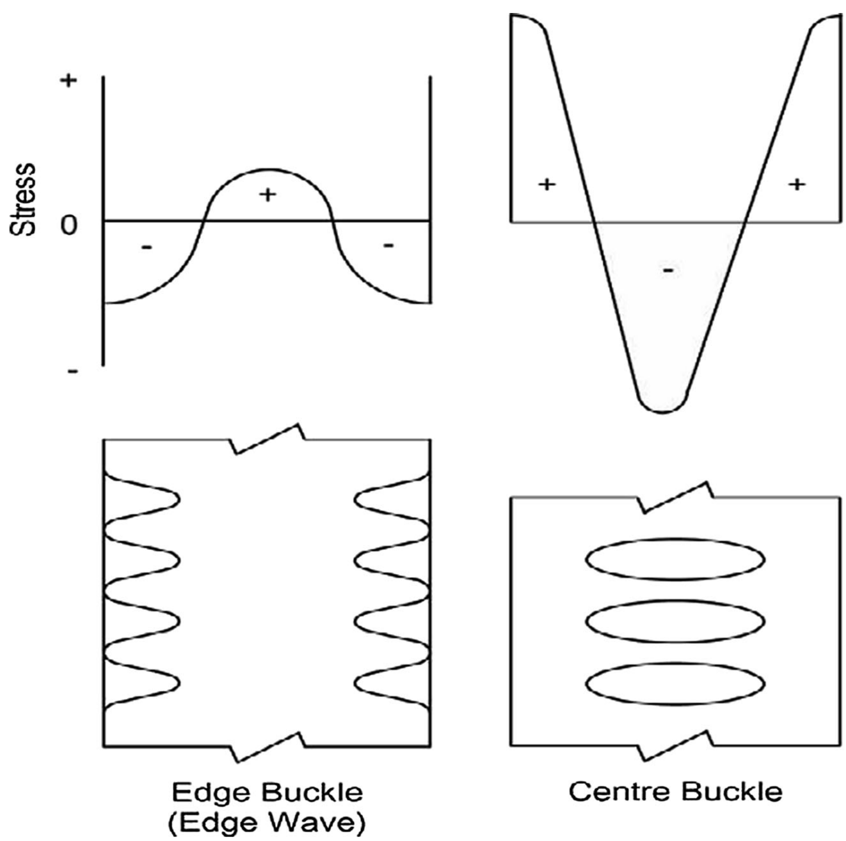

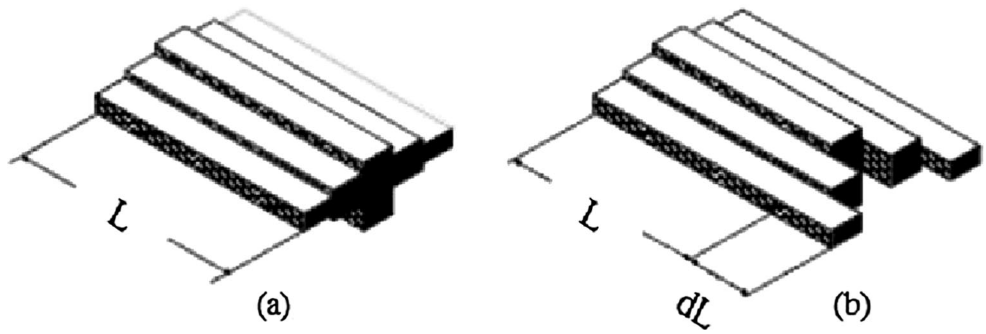


**Fig. 3** Longitudinal elongation after rolling with nonuniform reduction along the plate width **a** solid plate, **b** plate with collection of ribbons

a method to predict the strip profile as a result of roll deflection, and also, Wang et al. [15] investigated the effect of thermal stress on strip flatness.

Throughout this century, the rolling process has been analyzed by various analytical and numerical methods such as the slab method, the slip line method, the upper bound method, the boundary element method, and the finite element method. In comparison to the other methods of analyzing the rolling process, the finite element method is the most practical and accurate. Differences between models that have been proposed with using the FEM to investigate shape defects in rolling process are as follows:

1. The type of analysis (transient, steady-state);
2. The constitutive law for the material behavior (elastoplastic, rigid plastic);
3. The type of discretization (2D in the case of plane deformation, 3D); and
4. The type of analysis (mechanical, thermal) [16].

For example, Mori et al. [17] have developed a finite element method using the assumptions of rigid plastic and slightly compressible material to predict the velocity during isothermal steady and unsteady plane strain rolling conditions. Hwu and Lenard [18] have used a finite element method formulation for the rolling processes to assess the effects of work roll deformation and various friction conditions on strain distributions. Yarita et al. [19] have analyzed the plane strain rolling process utilizing an elastic-plastic finite element model. Fang et al. [20] have analyzed cross-wedge rolling process using 3D finite element model, and Jiang et al. [21] have simulated thin strip rolling with 3D finite element rigid plastic model.

Previous research in the fields of buckling of plate in flat rolling process are based on the assumption of plane strain along the entire width and dealt with the buckling analysis, employing some empirical relations for residual stresses according to the experiments and numerical estimates without considering the deformation of plate in the roll gap. This article investigates the distribution of longitudinal residual stresses due to the nonuniform thickness profile of the entry plate with consideration of all aspects of material flow and study the relation between the plate dimensions and the crown ratio changes for transition from a flat state to bad shape and compares the critical crown ratio changes between long edge shape and long middle shape.

## 2 Flatness defects in flat rolling

Flatness defects in rolled strip can take many forms, most of which are characterized by waves or ripples, extending over the entire width or confined to narrow portions of it. These are evidently the outcome of elastic buckling of the strip under the

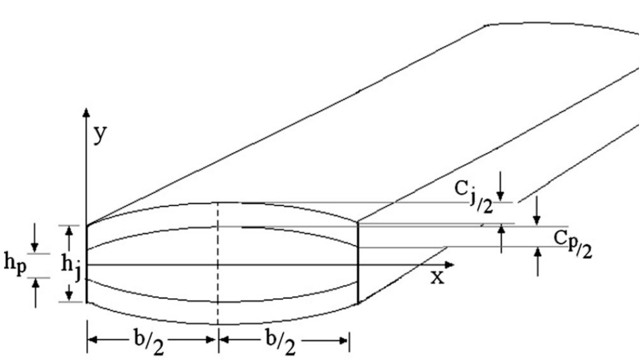


**Fig. 4** Typical positive crown

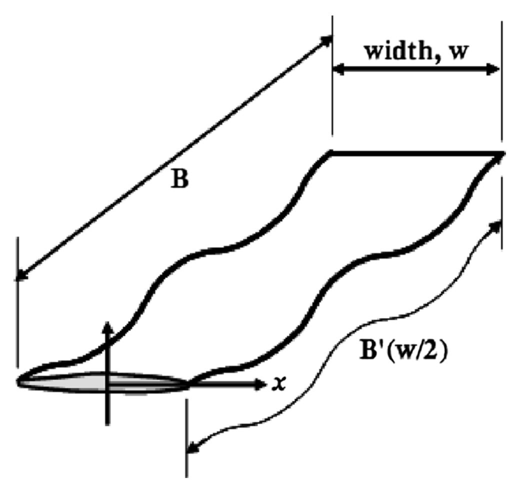


**Fig. 5** Strip flatness definition

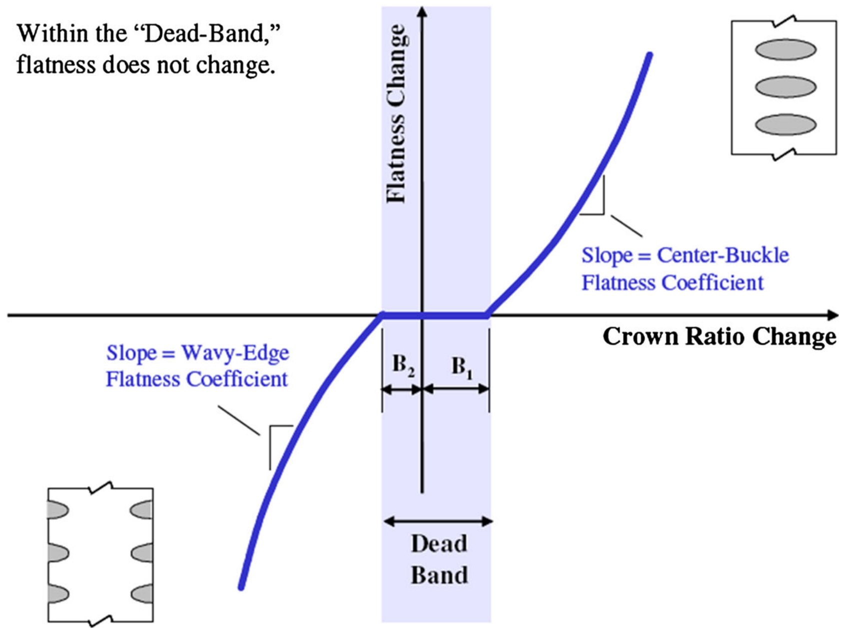


**Fig. 6** Strip flatness change as a function of crown ratio change

action of excessive compressive or shear stresses in the plane of the strip. The most typical flatness defects associated with the rolling process are center buckles and edge waves, which are depicted in Fig. 2 with a schematic representation of the longitudinal stress distribution along the plate width probably related to each case.

It is generally considered that edge waves and center buckles are associated with the lowest stress level and occur when the compressive residual stress distributed in the strip exceeds a certain limit. They are portrayed as the outcome of self-equilibrated distributions of stress, whereas other type of flatness defects like herringbone and quarter buckles are the outcome of more intricate stress patterns in hot or cold strip [22].

As stated earlier, longitudinal residual stresses will form in the plate as a cause of nonuniform deformation in width direction. Indeed, if imagine a plate as a collection of narrow ribbons which is over-rolled at the plate edges, according to Fig. 3b, the length of ribbons located at edges are higher than the ribbons located at the center. In fact, higher reduction at plate edge causes greater flow of material in the longitudinal direction in this region with respect to central part of strip.

In this state, considering a solid plate due to rigid motion of the plate after leaving the roll gap (Fig. 3a) and interaction with that of the nearby longitudinal elements (instead of ribbons), a group of elements that elongated larger than the others goes under compressive longitudinal stress to decrease in length, and those elements which are shorter are increased in length owing to longitudinal tensile stress; so, all elements reach to the same length. Accordingly, any factor that causes nonuniform material flow in the rolling direction across the plate width creates residual stress in plate.

In this order, rolling engineers are challenged to identify the range of acceptable strip crown value variations to prohibit the wavy edge or center buckle shape defects. According to Eq. 1, crown is the difference between the thickness at the center and the edges of the plate; it is considered positive when the center thickness is larger and negative when the center thickness is smaller. Figure 4 shows the typical crown used in rolling.

$$C = h_c - \frac{(h_{e1} + h_{e2})}{2} \quad (1)$$

where $h_c$ is the thickness at the center and $h_{e1}$ and $h_{e2}$ are the thickness at the two edges.

In most rolling operations, and particularly in hot rolling where strip thickness to width ratio is higher than thin cold strip rolling, the crown to thickness ratio variations (which are known as crown ratio variations) without affecting the flatness

**Table 1** Model geometries

| | |
|---|---|
| Roll | |
| Diameter | 400–500 mm |
| Length | 240–540 mm |
| Speed | 6 rad/s |
| Plate | |
| Width | 200–500 mm |
| Length | 2000 mm |
| Initial thickness | 4–2 mm |
| Final thickness | 3.5–1.5 mm |
| Crown | 0–0.4 mm |

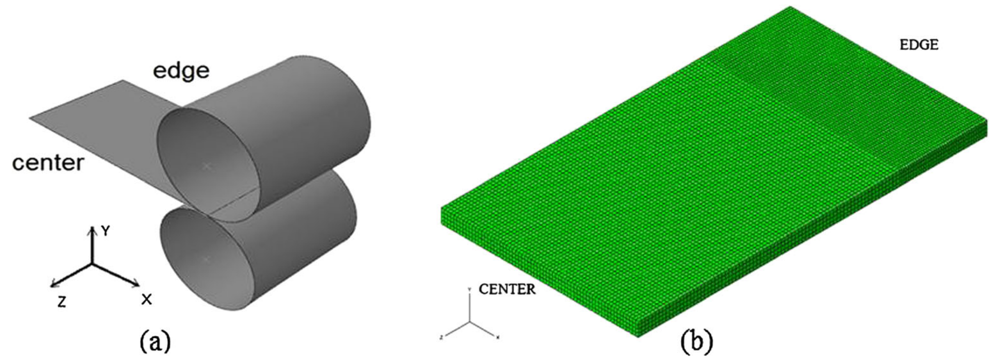


**Fig. 7** **a** Rolling model setup, **b** plate mesh configuration

is higher. Flatness is simply defined according to Eq. 2 with variables that are illustrated in Fig. 5.

$$F(x) = 10^5 \left[ B'(x) - B \right] \Big/ B \tag{2}$$

The range of crown ratio changes that does not affect the existing strip flatness is known as the flatness "deadband". Outside the deadband, strip flatness may change depending to the crown ratio change, as illustrated in Fig. 6. The deadband for a center buckle condition may be different from that of a wavy edge condition, as depicted by the quantities $B_1$ and $B_2$, respectively, in Fig. 6.

Though theoretically, it seems that it is desirable to roll all plates with zero crown, plate rollers experienced that a small positive crown is needed to keep plate track centrally through the roll gap. Generally, a minimum crown of about 0.08 mm for good tracking is considered. Townsend and Shohet [12] proposed a quantitative relationship between crown and flatness, which states that if there is no significant recovery or recrystallization after the jth pass, then the final plate should be flat if the following relationship (according to Shohet and Townsend [12]) is maintained:

$$-80\left(\frac{h_p}{b}\right)^2 < \left(\frac{C_j}{h_j} - \frac{C_p}{h_p}\right) < 40\left(\frac{h_p}{b}\right)^2 \tag{3}$$

As can be seen from Shohet and Townsend theory (Eq. 3), for no change in plate profile, no buckling will occur and the deadband for a wavy edge is larger than the center buckle. In the present paper, cold rolling process of strip is simulated using a conventional FE explicit code for different profile thickness to investigate the above relation and compare the deadband in formation of the wavy edge and center buckle condition.

## 3 Finite element model

The simulations were performed using ABAQUS/explicit [23] finite element code. A three dimensional (3D) FE model was developed to study the effect of uneven deformation on the residual stresses across the plate width and also to simulate the thickness profile changes across the plate width. In this modeling, thermal effects are not considered in order to simplify the model and better investigate special parameters that were the subject of this paper. Due to the symmetry of the problem and to reduce the computational time, only half of the geometry was simulated. Geometries of the plate and roll were created according to Table 1. Plate crown was simulated as an arc in thickness profile of plate and extruded over the length of plate.

Figure 7 shows the steady-state rolling model setup in which only half of the model was simulated and symmetry boundary conditions were applied to the center of plate and rolls. The edges of plate are free to deform and no tension applied to the plate; so, the plate is completely relaxed after rolling. The rolls which are rigid are fixed at specified distance from each other and rotate at defined velocity. Plate mesh configuration is also illustrated in Fig. 7 which has shown finer mesh at the plate edges as a cause of sensitive variations of stress and strain at this location.

In this study, material behavior is considered to be elastic-plastic, and the behavior of material in plastic state is only a function of plastic strain. So that the plastic properties of material and hardening parameters were supplied into the model using the Ludwick's stress-strain relationship (Eq. 4) where *n* and *k* are given in Table 2 which refers to AISI 1010

**Table 2** Steel properties [24]

| Steel (percentage) | k (MP) | *n* | Yield stress (MP) | Young modulus (GP) |
|---|---|---|---|---|
| 0.004N 0.32Si 0.022S 0.01P 0.31Mn 0.13C | 716 | 0.2 | 300 | 200 |

**Table 3** Comparison between simulation and theoretical results

| Roll stand | | FEM | | Bland and ford | | Error% | |
|---|---|---|---|---|---|---|---|
| Dimension (mm) | | F (KN) | T (KN.m) | F (KN) | T (KN.m) | F | T |
| hp: 1.5<br>r: 250 | hj: 2<br>b: 200 | 840 | 3.95 | 767 | 4.16 | 8.69 | 5.05 |
| hp: 1.5<br>r: 250 | hj: 2<br>b: 400 | 1640 | 7.9 | 1536 | 8.34 | 6.34 | 5.28 |
| hp: 3<br>r: 250 | hj: 4<br>b: 200 | 1085 | 7.22 | 992 | 7.65 | 8.57 | 5.62 |
| hp: 3<br>r: 150 | hj: 4<br>b: 200 | 800 | 4.14 | 730 | 4.38 | 8.75 | 5.48 |

steel grade. Boundary conditions were imposed according to information obtained from the process plant.

$$\overline{\sigma} = k\overline{\varepsilon}^{n} \tag{4}$$

In this simulation, Lagrangian formulation is used for its better ability in studying the free surfaces in addition to contact surfaces. The penalty method is used for definition of contact conditions where friction is an important factor in this method; so, Coulomb friction model is used in this study with friction factor that was used by the manufacture. The elements used for the plate were C3D8R to simulate a deformable solid. These elements include reduced integration with stiffness hourglass control for improved stability and convergence. Due to large variation of strains and stresses at the edge of the plate, finer mesh was considered for a narrow band at the plate edges, and in order to uphold an acceptable aspect ratio for the elements, depending on the plate width, 350,000–600,000 elements were used. The rolls were simulated as an analytical rigid surface with R3D4 element.

To obtain reliable and accurate predictions concerning the residual longitudinal stresses, which are essential for the analysis of flatness defects caused by compressive residual stresses, the simulation regime has to be extended far enough outside the roll bite. This critical distance, measured in units of the projected roll gap length, can be reduced significantly by imposing the homogeneity of the strip velocity in rolling direction. Hence, at the beginning of simulation, the rolls are moved toward the plate to compress the plate, and then, the rolls speed up with certain acceleration. Starting simulation using this method leads to obtain reliable prediction of residual stress that generates as a cause of nonuniform deformation at distance of half the plate width from rolling area which stress distribution is constant.

In order to accelerate the simulation process, the use of a mathematical artifact (mass scaling) was adopted. Setting the mass scaling parameter to 1 results in the real interaction between the dynamic effects and the static loads applied to the system, but the simulations are too slow and time-consuming. A value of 200 was determined to be an optimum mass scaling parameter which satisfies the energy conditions in which the kinetic energy should be less than 10 % of the total internal energy.

After simulating the process, to verify the model, the rolling force and torque from the simulation were compared

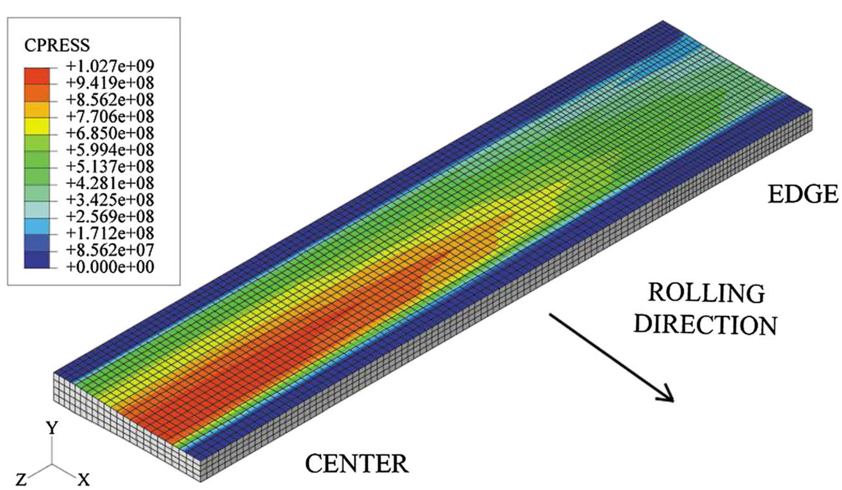


**Fig. 8** Distribution of roll pressure along plate width

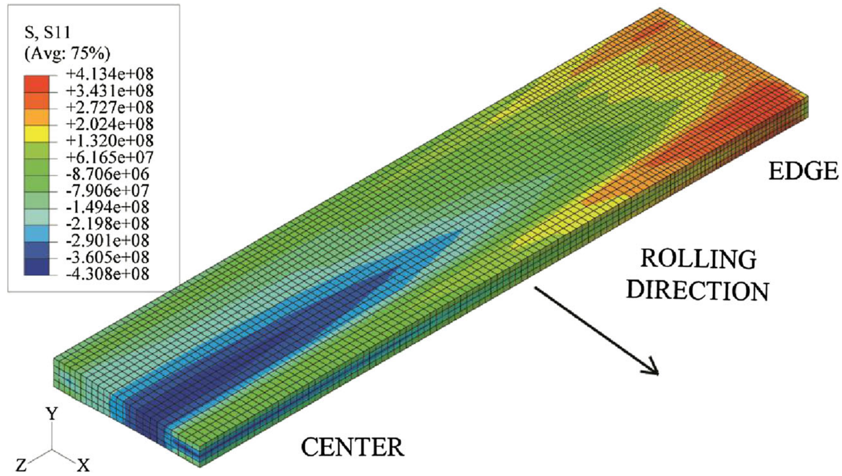


**Fig. 9** Contour of longitudinal stress in roll gap

with the theoretical values from the Bland and Ford [25] as given in Table 3. Comparison of roll force and torque shows that the differences between these two methods are less than 9 % which is due to many simplifying assumption being considered in the theoretical model. It is concluded that the provided model has an acceptable accuracy in studying rolling process.

## 4 Results and discussions

### 4.1 Rolling of plate with uniform profile

Review of the results from the simulation shows a nonuniform deformation of the plate across the width, while the reduction applied to the plate is uniform. In this state, owing to different boundary condition along the plate width, the distribution of transversal strain is not uniform, so that as a cause of symmetric condition at the center of plate and greater resistance to transversal flow of material, almost no transversal strain occurs in this region, while at the plate edges, material is free to flow in transversal direction. Additionally, these conditions lead to variation of flow stress along the plate width so that as represented in Fig. 8, nonuniform distribution of roll pressure is created.

Due to variation of roll pressure along the plate width, the frictional stress change and consequently the shear strain in x-y plane attain different values across the plate width. Because of the same effect of shear strain and transversal flow on the longitudinal flow of material, longitudinal displacement of material at central region of the plate is larger than the edges, so that the longitudinal stress generates in order to uniform the plate velocity at exit of the roll gap. As represented in Fig. 9, the longitudinal compressive stress at the center of the plate, where the shear strain is greater and the transversal flow is negligible, is generated.

Nonuniform distribution of longitudinal stress in transverse direction at entry to or exit from the roll gap causes

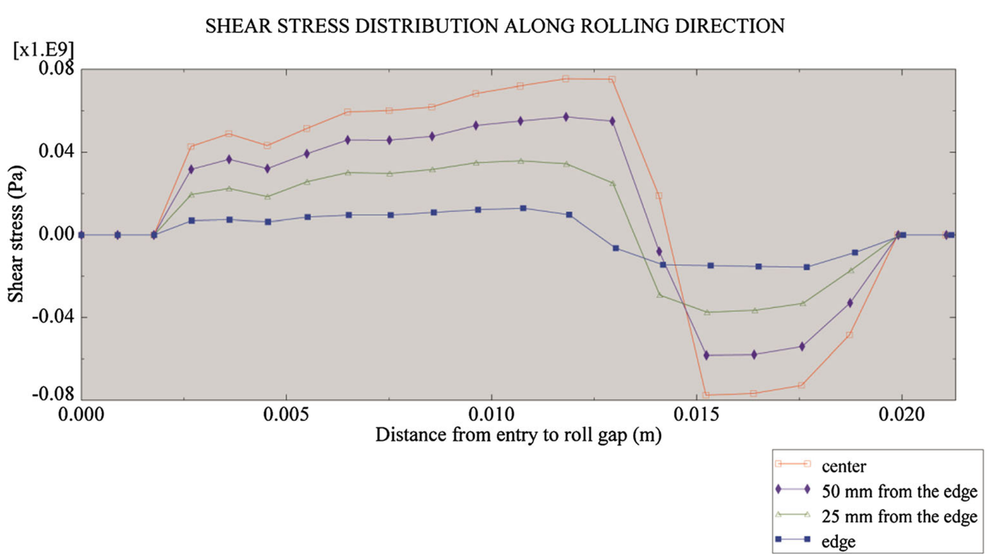


**Fig. 10** Neutral plane along the plate width

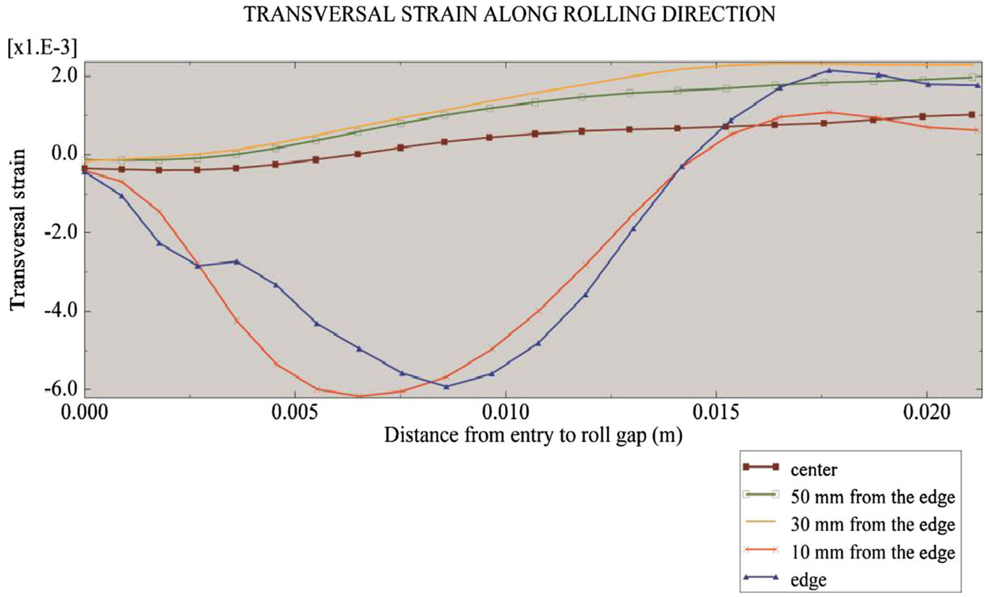


**Fig. 11** Transverse strain variation at different location

nonuniform displacement of neutral plane (where the velocity of the plate is equal to that of the roll surface velocity) along the rolling direction due to changes in rolling force per unit width. As illustrated in Fig. 10, the front tension at edges causes the neutral plane to move backwards and in contrary, compressive stress at central region of the plate move the neutral plane forwards along the rolling direction. Nonuniform displacement of the neutral plane leads to non-uniform distribution of longitudinal velocity of the plate at entry and exit of the roll gap along the plate width. This heterogeneity of the velocity along the plate width deforms the plate prior to entry and after leaving the roll gap.

After leaving the roll gap, noticeable variation in longitudinal stress occurs that may not be considered as a cause of nonuniform velocity distribution as the main reason. Studies on the transversal strain variations at the edges indicate that special flow of material at this region affects the longitudinal stress severely. In this state, due to the effect of tensile stress at the plate edges which are free to flow in transversal direction, the deformation condition is similar to simple tension, and this leads to local contraction at this region as illustrated in Fig. 11.

Severe decrease in transversal strain at the edges increases the metal flow in rolling direction. With regard to the longitudinal tensile stress at this region, permanent deformation of longitudinal plastic strain in this area is increased. As it can be seen in Fig. 12, the longitudinal plastic strain in a narrow ribbon at the edges is higher than the other location along the plate width. Comparison of the final plastic strain and the residual strain in rolling direction in Fig. 12 shows that the variations in longitudinal stress along the rolling direction

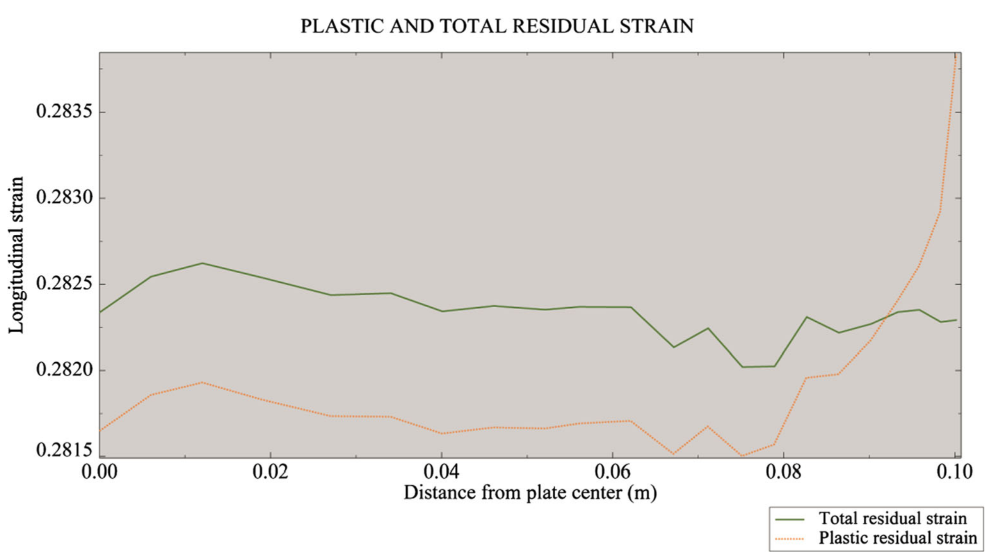


**Fig. 12** Comparison of longitudinal plastic strain and total strain

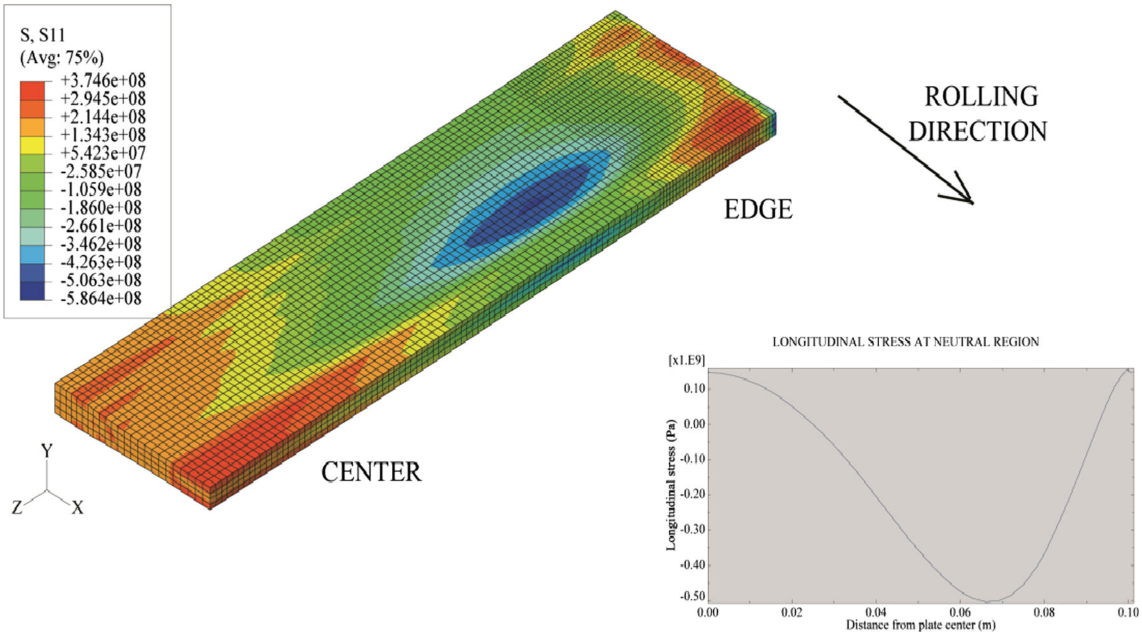


**Fig. 13** Contour of longitudinal stress distribution in the roll gap

after leaving the roll gap create a uniform distribution of longitudinal strain along the plate width such that the elastic compressive strain at the plate edges is generated and in other locations in the transverse direction, elastic tensile strain is originated. Generation of compressive stress at the plate edges creates edge waves in the final product.

## 4.2 Rolling of plate with negative crown

In rolling of plate with negative crown, the plate at the edges is thicker than the center so that a greater reduction at edges is required to achieve a uniform thickness at exit. According to previous research in this field including the Shohet and Townsend [12], as a cause of more reduction at plate edges, material flow in longitudinal direction increases, and due to rigid motion of plate after exit from the roll gap, longitudinal compressive stress is generated at this region and the edge waves are created.

Simulation results in Fig. 13 present a relatively different distribution of longitudinal stresses in comparison to what was predicted by Townsend and Shohet [12]. As it can be seen in Fig. 13, tensile longitudinal stress is applied in a narrow ribbon along the plate edge dissimilar the existing theories. In fact, under the effect of other factors such as nonuniform transversal flow and shear deformation, the maximum longitudinal strain rate is located at a certain distance from the edge.


**Fig. 14** Transversal strain distribution across plate width

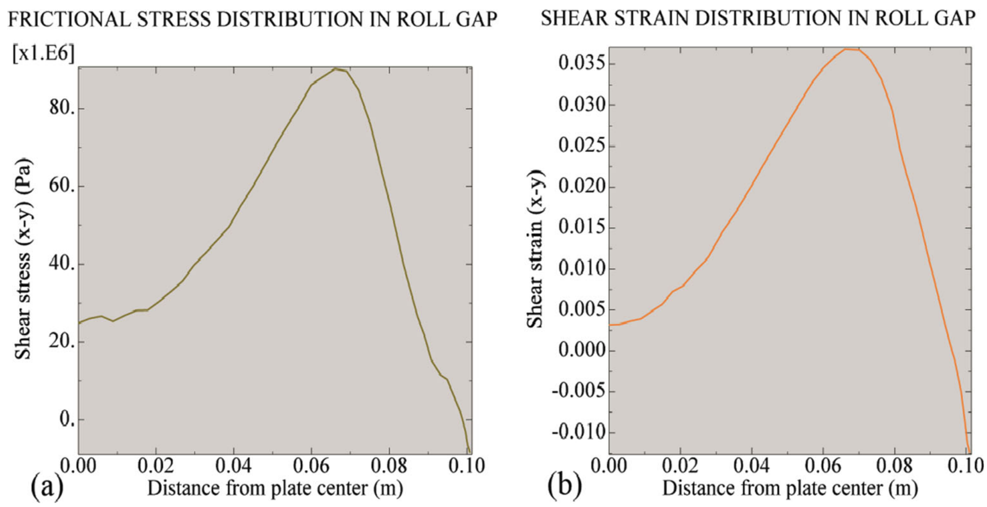


**Fig. 15** Distribution of shear stress and shear strain in x-y plane along plate width

This state is observed in other research work including Montmitonne [26] in rolling of plate with negative crown, but the reason for such behavior is not given.

This longitudinal stress distribution is reasonable when considering the different deformation condition along the plate width that leads to a nonuniform flow of material in transversal direction. As it is seen in Fig. 14, the transversal strain from the center to the plate edges increases due to changing of the boundary condition from plane strain at the center to the plane stress at the edges. In addition, as a cause of nonuniform distribution of roll pressure, shear stress is not uniform along the plate width which leads to larger shear strain in the plane of x-y at a certain distance from the edges as seen in Fig. 15. Under the same effect of these nonuniformities on the longitudinal flow of material, maximum longitudinal displacement is located at a certain distance from the edges so that in order to uniform the longitudinal flow of material, compressive stress is presented at this region.

Another important deformation that influences the longitudinal stress distribution is the variation of transversal strain along the plate edges. According to Fig. 16, transversal strain variation along the edge is different from the other locations along the plate width. This phenomenon is caused by the tensile stress and plane stress condition at this point that causes local necking at this region and creates larger longitudinal plastic strain as illustrated in Fig. 17. So, elastic deformation in plate occurs after it leaves the roll gap to maintain a uniform distribution of the longitudinal strain as it can be seen in Fig. 17. In this state, tensile stress is replaced by compressive stress at the edge and increase the possibility of buckling in this region.

### 4.3 Rolling of plate with positive crown

Considering a plate with positive crown, thickness at the plate center is larger than the edges, and hence, greater reduction at

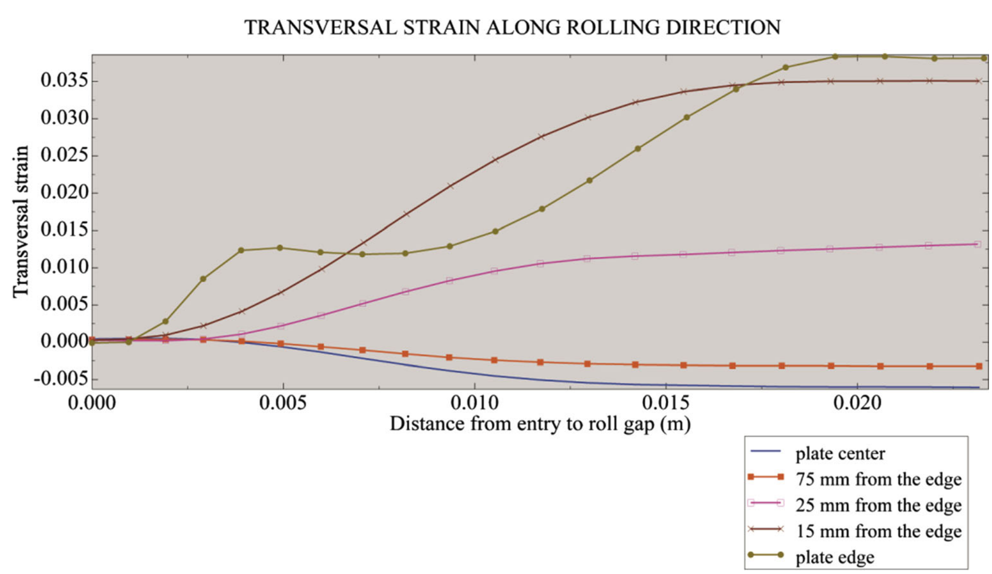


**Fig. 16** Variation of transversal strain along the rolling direction

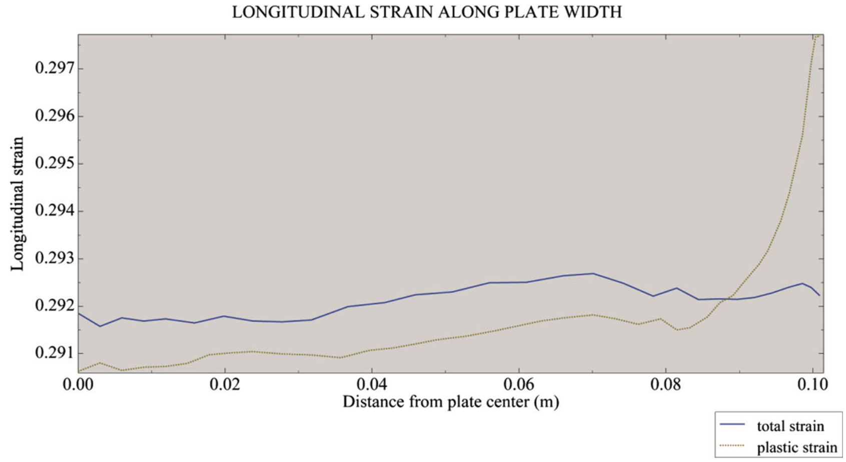


**Fig. 17** Distribution of longitudinal strain along the plate width

the center is required to achieve a uniform thickness at exit. In this condition, due to larger thickness strain at the center, the longitudinal flow of material is greater than the other points across the plate width, and hence according to Townsend and Shohet theory, elastic deformation occurs in the plate to resist against larger longitudinal strain at central region, and hence, compressive stress is created in this region while tensile stress is presented at the edges to increase the material flow along the rolling direction at these locations.

Investigation on simulation results shows that unlike the earlier condition (rolling of plate with negative crown), simulation results are in agreement with the theory of Townsend and Shohet. It may be concluded that the variations of transverse and shear deformation have the same effect on the longitudinal stress as the positive crown deformation. According to Fig. 18, longitudinal stress in the middle of plate is compressive as expected, and tensile stress is applied at the plate edge in order to maintain the rigid body motion of plate after leaving the roll gap.

Transversal strain distribution in Fig. 19a shows that variation of transversal strain in plate with positive crown is different from that of the plate with negative crown. Indeed, changing the crown sign leads to changing the transversal flow direction so that in the central region due to larger reduction in plate thickness, metal flow in rolling direction increases and causes greater resistance against longitudinal flow of material, and hence as a result of compressive stress in this region, transversal flow of material leads to increase the width of plate while the edges of plate as a cause of less longitudinal flow is under tensile stress and compress in the transversal direction. So, referring to Fig. 19b, the longitudinal strain is greater in the central region as expected.

Comparison of the total strain and the plastic strain in rolling direction shows that variation of longitudinal strain

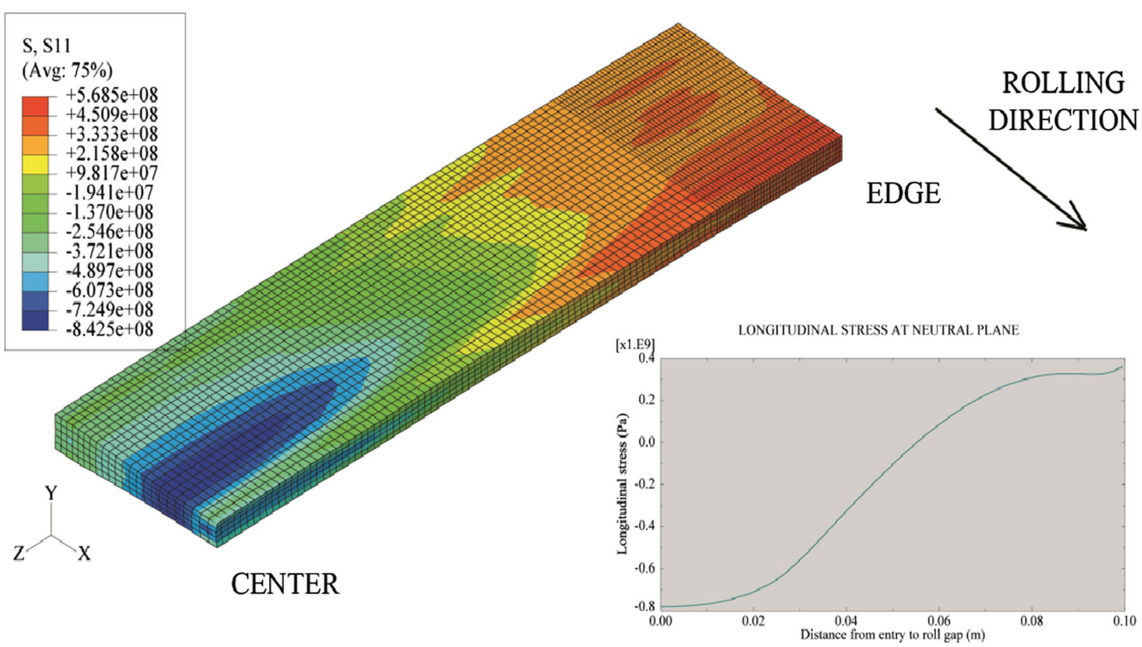


**Fig. 18** Contour of longitudinal stress distribution in the roll gap

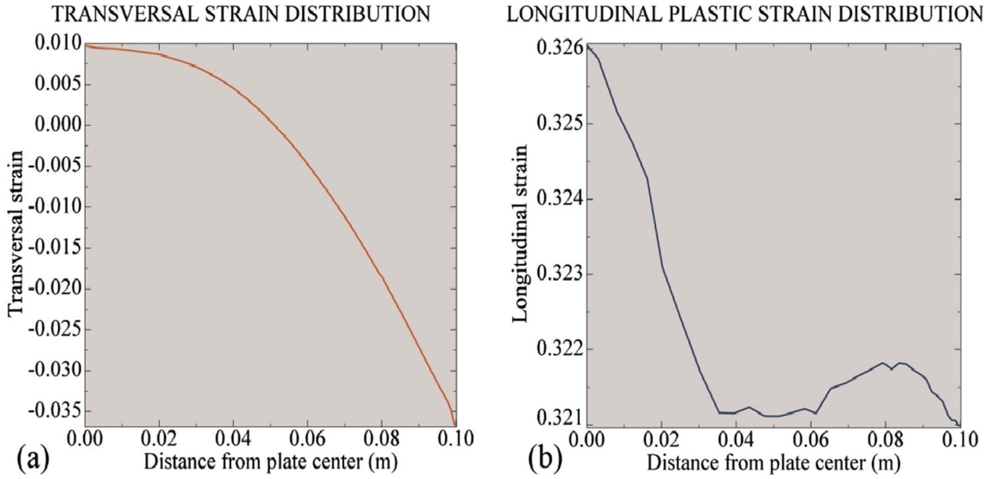


**Fig. 19** Distribution of **a** transversal strain and **b** longitudinal plastic strain at exit

after removal from the roll gap is dissimilar to that of the plate rolled with negative crown and final distribution of the longitudinal strain is not uniform as illustrated in Fig. 20. This is partly due to the velocity difference along the plate width at the output from roll gap.

According to Fig. 21, the difference between compressive and tensile stress along the plate width for positive crown profile is greater than the negative crown profile due to the similar effect of transversal flow on the longitudinal strain, and hence, the value of this difference is greater, and accordingly, displacement of the neutral zone along the rolling direction is larger. This causes to increase the velocity difference between the center and the edges. Here, with respect to tensile stress at the edge, the neutral zone is moved backwards. By increasing the neutral plane thickness, the plate velocity at entry to and exit from the roll gap increases, and in contrary, in the central region, the opposite effect will occur. To obtain a uniform distribution of velocity at exit from the roll gap, the longitudinal strain will decrease at the edges due to larger longitudinal velocity at this point.

### 4.4 Comparison of the effect of positive and negative crown on deformation

Results obtained from simulation show that transversal flow is dependent on the crown sign of the plate. As depicted in Fig. 22a, transversal flow change with crown's sign and transversal strain distribution changes in the central region of the plate are less in comparison to the plate edge due to higher friction force and pressure in transversal direction, In fact, transverse flow at the edge of the plate is higher.

According to Fig. 22b, transversal flow of material in rolling of plate with a positive crown tends to reduce the plate width as a result of larger transversal compressive strain, whereas transversal flow of plate with negative crown tends to increase the plate width due to larger transversal tensile strain at plate edges. This behavior is reported in an analytical method by Dixon and Yuen [27] as illustrated in Fig. 23.

From the transversal strain distribution, it is concluded that the longitudinal flow of material for a plate with initial positive crown is larger than the negative crown, and hence as it is

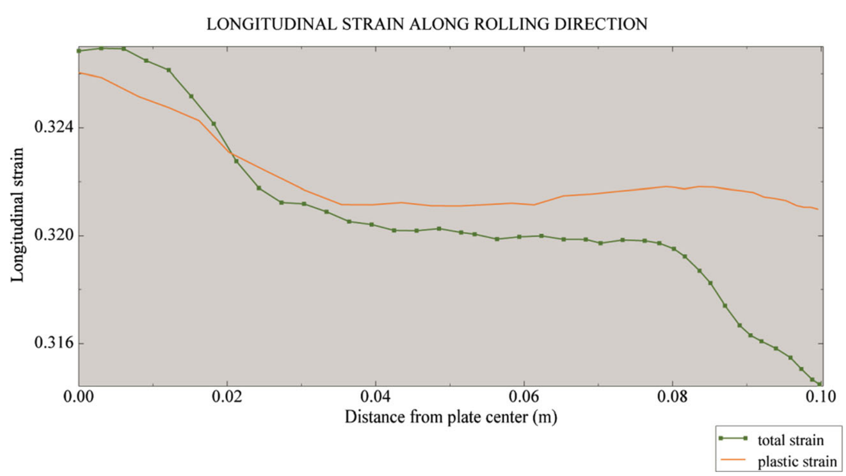


**Fig. 20** Comparison between residual strain and plastic strain in rolling direction

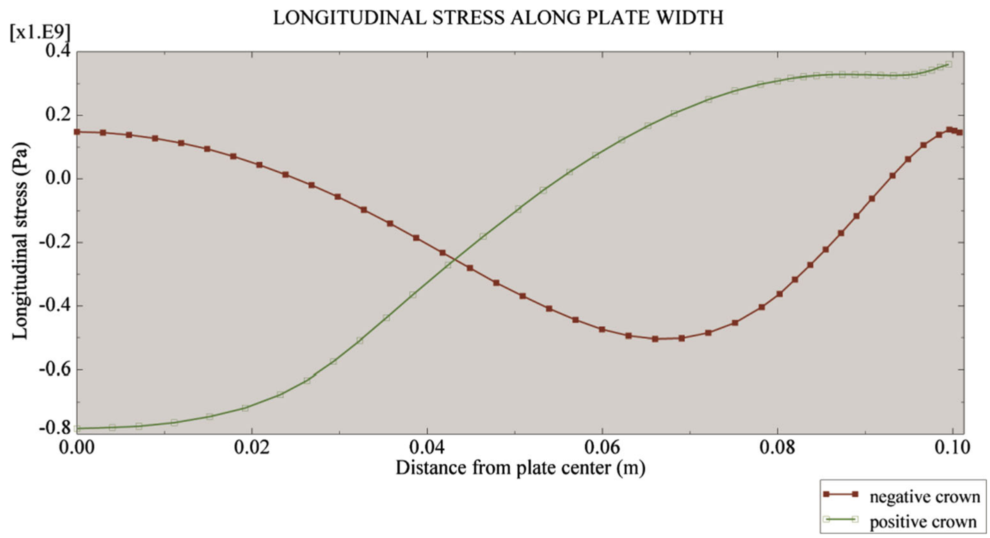


**Fig. 21** Distribution of longitudinal stress for different crown sign

seen in Fig. 24, larger longitudinal strain is created in plate with initial positive crown, and as a result of that, differences in longitudinal flow between center and edge of plate are greater, and this phenomena cause larger longitudinal stress to uniform the material flow in longitudinal direction across the width as depicted in Fig. 21.

Investigation on longitudinal residual stress for equal crown and different sign as shown in Fig. 25 shows that the magnitude of the compressive stress for negative crown is larger due to necking phenomena at the plate edges. In fact, the transversal strain changes at the edge for the negative crown plate have led to increase of differences of longitudinal strain between edge and center of the plate, whereas these changes for positive crown have an opposite effect. Besides, as a cause of larger difference of output velocity across the plate width for a positive crown plate, nonuniform longitudinal residual stress is created in the final product. Due to the residual stress distribution, buckling of a plate with a negative crown is more probable than a plate with a positive crown.

### 4.5 Checking the validity of Townsend and Shohet theory

In order to investigate the relation between the relative crown and plate dimension for transition of plate shape from flat state to bad shape and make a comparison with Shohet and Townsend relation (Eq. 3), various runs with different dimension and relative crown (according to Appendix A) are created, and the final plate shapes were investigated.

Analysis of simulation results as shown in Fig. 26 and comparison with the Townsend and Shohet relation show differences between these two methods. In fact, Shohet and Townsend results due to eliminating of transversal flow of material in their calculations could not explain the relation between thickness profile changes and the final plate shape as

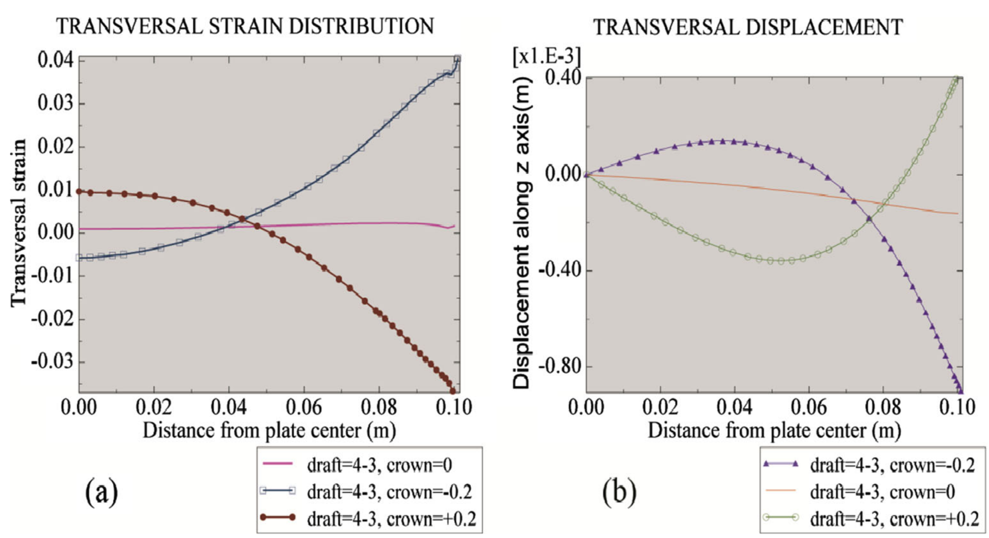


**Fig. 22** Comparison of **a** transversal strain, **b** transversal displacement for different profile thickness

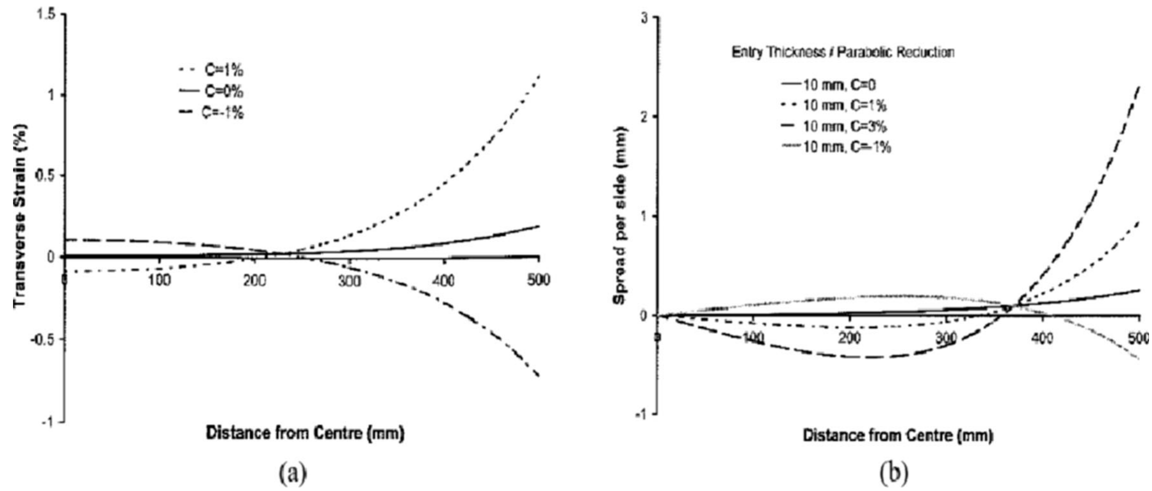


**Fig. 23** Comparison of **a** transversal strain, **b** transversal displacement for different profile thickness under rolling process for 40 % reduction and initial thickness of 10 mm [27]

**Fig. 24** Comparison of plastic longitudinal strain for different profile thickness

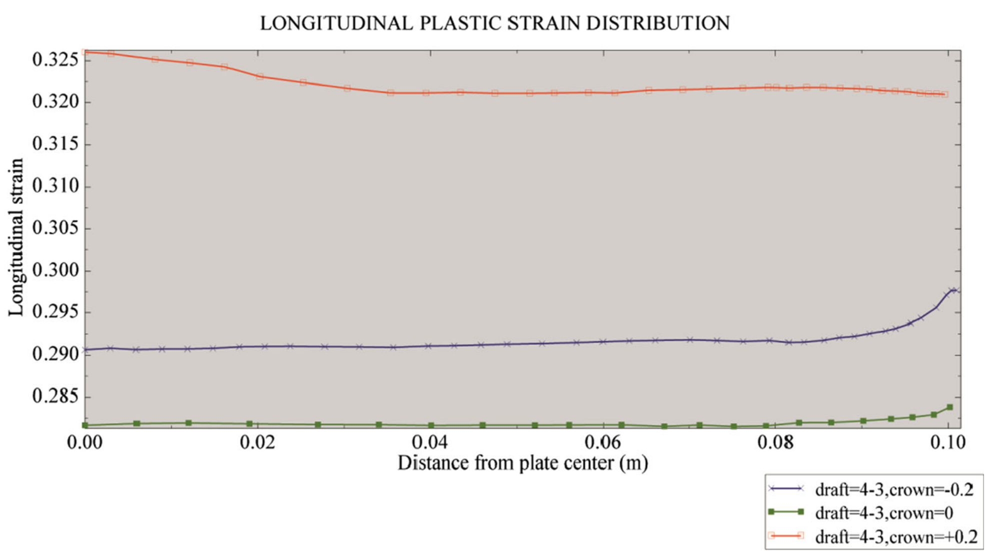


**Fig. 25** Comparison of longitudinal residual stress between negative and positive crown

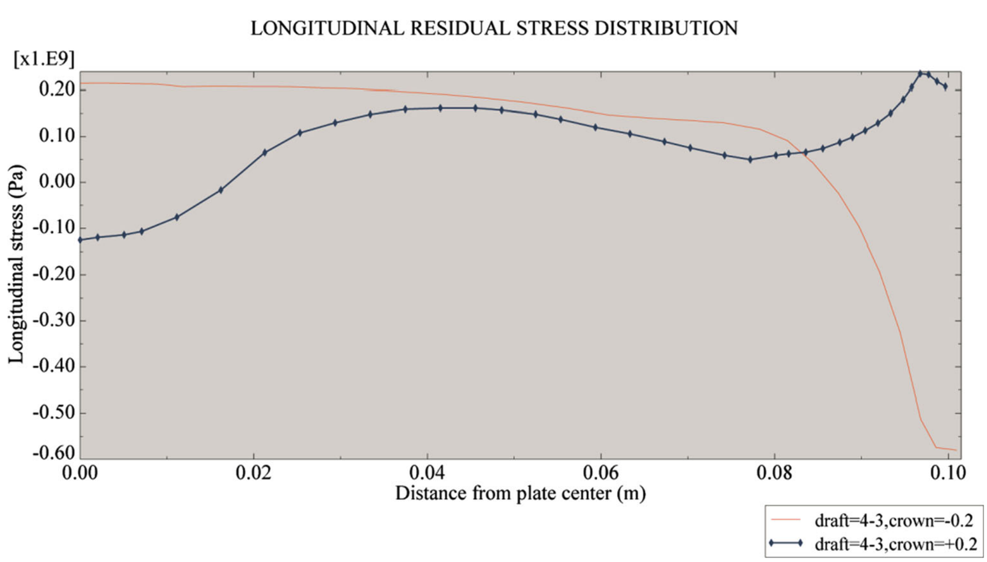

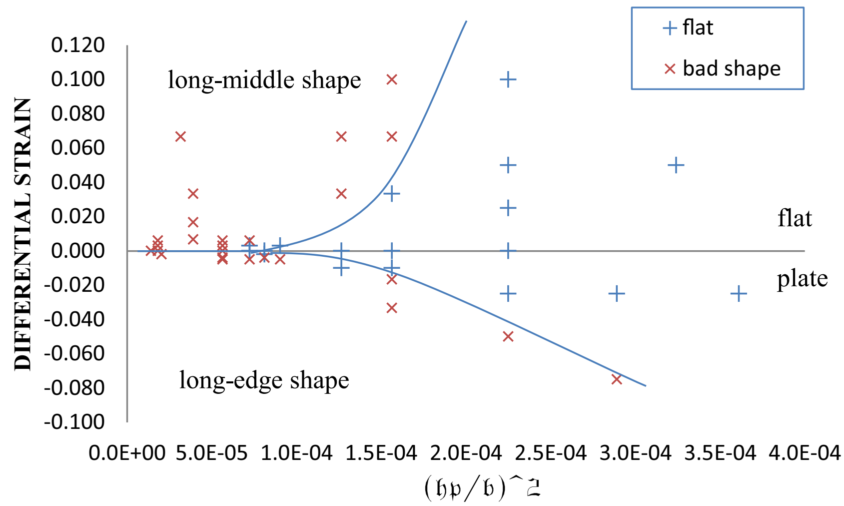


**Fig. 26** Relation between crown changes and plate dimension showing the transition from flat to bad shape

accurate as the simulation results. Fundamental differences between these two methods can be summarized as follows:

1. Due to transversal flow of material in the roll gap, in contrast with Shohet and Townsend theory, buckling occurs in rolling of plate with zero crown changes. This occurs in rolling of plate with very small ratio of output thickness into plate width that nonuniform deformation of plate as a result of different boundary condition across the plate width has a great influence on residual stresses.
2. According to simulation results, the plate resistance against the center buckling is higher than the edge wave. In fact, as stated earlier, residual compressive stress in rolling of plate with a positive crown is smaller than that of a negative crown and also based on the research about the critical threshold for various buckling patterns [28] (Fig. 27), the buckling load for center wave case is larger than the edge wave case.
3. By increasing the of ratio of the output thickness into the plate width, the range of allowable thickness profile variations will increase with a greater slope; this is not in agreement to the Shohet and Townsend theory.

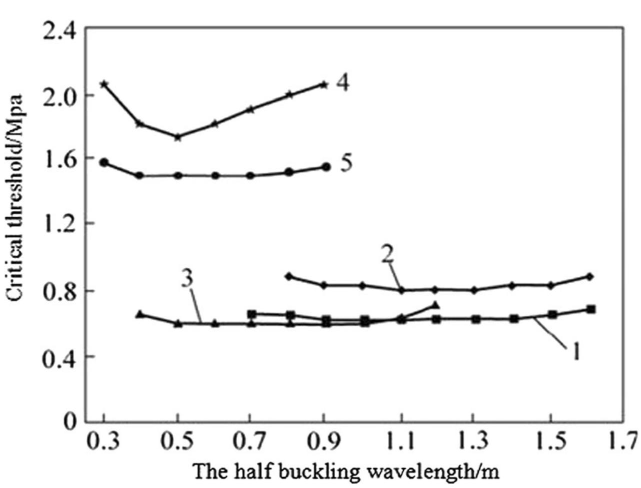


**Fig. 27** Comparison of buckling load for different case: (1) edge wave, (2) center wave, (3) symmetrical buckling, (4) center buckling with edge wave, (5) quarter buckling [28]

## 5 Conclusion

In this research, causes of formation of shape defects in flat rolling product are studied, and it is shown that the nonuniform deformation along the plate width leads to formation of longitudinal stress.

To study the effect of the nonuniformity on flatness of the plate, a simulation model for the process is created using conventional finite element software. It is found that in addition to uneven geometrical factor influencing the plate quality, variation of forming condition along the plate width as a result of different boundary condition leads to heterogeneity of deformation despite the fact that variation in residual stresses may be very low. It is shown that this condition plays an important role in buckling of thin flat products.

Additionally, it is shown that the transition from flat condition to bad shape for specific ratio of output thickness to the width of plate occurs as a result of thickness profile changes, and also, it has shown that critical crown ratio changes for long edge shape are smaller than long middle shape.

Investigations for validity of Townsend and Shohet theory were made. It is shown that Townsend and Shohet results are not able to predict the shape defect as accurate as the FE simulation due to eliminating of transversal flow of material in their calculations.

## Appendix A

**Table 4** Results for different plate dimension

| Sheet number | b (mm) | hj (mm) | hp (mm) | cj (micrometer) | (hp/b)^2 | $e_t$[a] | Shape[b] |
|---|---|---|---|---|---|---|---|
| 1 | 200 | 2 | 1.5 | 0 | 0.000056 | 0.000 | B |
| 2 | 200 | 2 | 1.5 | 6 | 0.000056 | 0.003 | B |
| 3 | 200 | 2 | 1.5 | −8 | 0.000056 | −0.004 | B |
| 4 | 200 | 2 | 1.5 | −10 | 0.000056 | −0.005 | B |
| 5 | 200 | 2 | 1.5 | 12 | 0.000056 | 0.006 | B |
| 6 | 400 | 2 | 1.5 | 0 | 0.000014 | 0.000 | B |
| 7 | 200 | 2 | 1.7 | 0 | 0.000072 | 0.000 | F |
| 8 | 400 | 2 | 1.7 | 0 | 0.000018 | 0.000 | B |
| 9 | 200 | 2 | 1.7 | 6 | 0.000072 | 0.003 | F |
| 10 | 400 | 2 | 1.7 | 6 | 0.000018 | 0.003 | B |
| 11 | 200 | 2 | 1.7 | −10 | 0.000072 | −0.005 | B |
| 12 | 200 | 2 | 1.7 | 12 | 0.000072 | 0.006 | B |
| 13 | 400 | 2 | 1.7 | 12 | 0.000018 | 0.006 | B |
| 14 | 200 | 2 | 1.8 | 0 | 0.000081 | 0.000 | F |
| 15 | 200 | 2 | 1.8 | −4 | 0.000081 | −0.002 | F |
| 16 | 400 | 2 | 1.8 | −4 | 0.000020 | −0.002 | B |
| 17 | 200 | 2 | 1.8 | −8 | 0.000081 | −0.004 | B |
| 18 | 200 | 2 | 1.9 | −10 | 0.000090 | −0.005 | B |
| 19 | 200 | 2 | 1.9 | 6 | 0.000090 | 0.003 | F |
| 20 | 200 | 3 | 2.25 | 0 | 0.000127 | 0.000 | F |
| 21 | 200 | 3 | 2.25 | −30 | 0.000127 | −0.010 | F |
| 22 | 200 | 3 | 2.25 | 100 | 0.000127 | 0.033 | B |
| 23 | 200 | 3 | 2.25 | 200 | 0.000127 | 0.067 | B |
| 24 | 400 | 3 | 2.25 | 200 | 0.000032 | 0.067 | B |
| 25 | 200 | 3 | 2.5 | 0 | 0.000156 | 0.000 | F |
| 25 | 200 | 3 | 2.5 | −30 | 0.000156 | −0.010 | F |
| 26 | 200 | 3 | 2.5 | −50 | 0.000156 | −0.017 | B |
| 27 | 200 | 3 | 2.5 | −100 | 0.000156 | −0.033 | B |
| 28 | 200 | 3 | 2.5 | 100 | 0.000156 | 0.033 | F |
| 29 | 200 | 3 | 2.5 | 200 | 0.000156 | 0.067 | B |
| 30 | 200 | 3 | 2.5 | 300 | 0.000156 | 0.100 | B |
| 31 | 400 | 3 | 2.5 | 20 | 0.000039 | 0.007 | B |
| 32 | 400 | 3 | 2.5 | 50 | 0.000039 | 0.017 | B |
| 33 | 400 | 3 | 2.5 | 100 | 0.000039 | 0.033 | B |
| 34 | 200 | 4 | 3 | 0 | 0.000225 | 0.000 | F |
| 35 | 200 | 4 | 3 | −100 | 0.000225 | −0.025 | F |
| 36 | 200 | 4 | 3 | −200 | 0.000225 | −0.050 | B |
| 37 | 200 | 4 | 3 | 100 | 0.000225 | 0.025 | F |
| 38 | 200 | 4 | 3 | 200 | 0.000225 | 0.050 | F |
| 39 | 200 | 4 | 3 | 400 | 0.000225 | 0.100 | F |
| 40 | 200 | 4 | 3.4 | −100 | 0.000289 | −0.025 | F |
| 41 | 200 | 4 | 3.4 | −300 | 0.000289 | −0.075 | B |
| 42 | 200 | 4 | 3.6 | 200 | 0.000324 | 0.050 | F |
| 43 | 200 | 4 | 3.8 | −100 | 0.000361 | −0.025 | F |

[a] Differential strain

[b] F denotes flat specimens and B denotes buckled specimens

## References


1. Wang XD, Li F, Wang L, Zhang XL, Dong LJ (2012) Development and application of roll contour configuration in temper rolling mill for hot rolled thin gauge steel strip. Ironmak Steelmak 39:163–170
2. Shigeru T, Yoichi K, Kenji M (2009) Flatness control system of cold rolling process with pneumatic bearing type shape roll. Eng rev 42: 54–60
3. Wistreich JG (1968) Control of strip shape during cold rolling. J Iron Steel Inst 206:1203–1206
4. Shohet KN, Townsend NA (1968) Roll bending methods in crown control in four-high plate mills. J Iron Steel Inst 206:1088–1098
5. Sabatini B, Yeomans KA (1968) An algebra of strip shape and its application to mill scheduling. J Iron Steel Inst 206:1207–1213
6. Tarnopolskaya T, Hog FR (1998) An efficient method for strip flatness analysis in cold rolling. Math Eng Ind 7:71–95
7. Komori K (1998) Analysis of cross and vertical buckling in sheet metal rolling. Int J Mech Sci 40:1235–1246
8. Fischer FD, Rammerstorfer FG, Friedl N, Wieser W (2000) Buckling phenomena related to rolling and leveling of sheet metal. Int J Mech Sci 42:1887–1910
9. Fischer FD, Rammerstorfer FG, Friedl N (2003) Residual stress-induced center wave buckling of rolled strip metal. ASME J Appl Mech 70:84–90
10. Fischer FD, Rammerstorfer FG, Friedl N (2005) A study on the buckling behavior of strips and plates with residual stresses. Steel res int 76:327–335
11. Zhou Z, Lam Y, Thomson PF, Yuen DDW (2007) Numerical analysis of the flatness of thin, rolled steel strip on the run out table. J Eng Manuf 221:241–254
12. Townsend NA, Shohet KN (1971) Flatness control in plate rolling. J Iron Steel Inst 209:769–775
13. Hu YU, Gong DY, Jiang ZY, Xu JZ, Zhang DH, Liu XH (2009) Effect of initial crown on shape of hot rolled strip. J Iron Steel Res Int 16:32–34
14. Malik AS, Grandhi RV (2008) A computational method to predict strip profile in rolling mills. J Mater Process Technol 206:263–274
15. Wang X, Yang Q, He A (2008) Calculation of thermal stress affecting strip flatness change during run-out table cooling in hot steel strip rolling. J Mater Process Technol 207:130–146
16. Galantucci LM, Tricarico L (1999) Thermo-mechanical simulation of a rolling process with an FEM approach. J Mater Process Technol 93: 494–501
17. Mori K, Osakada K, Oda T (1982) Simulation of plane-strain rolling by the rigid-plastic finite element method. Int J Mech Sci 24:519–527
18. Hwu Y, Lenard JG (1988) A finite element study of at rolling. Trans ASME J Eng Mater Technol 110:22–26
19. Yarita I, Mallett RL, Lee EH (1988) Stress and deformation analysis of plane strain rolling process. Steel Res 56:231–255
20. Fang G, Lei LP, Zeng P (2002) Three-dimensional rigid-plastic finite element simulation for the two-roll cross-wedge rolling process. J Mater Process Technol 129:245–249
21. Jiang ZY, Tieu AK, Zhang XM, Lu C, Sun WH (2003) Finite element simulation of cold rolling of thin strip. J Mater Process Technol 140: 542–547
22. Zhou Z, Lam Y, Thomson PF, Yuen DDW (2007) Predicting quarter-buckling and herringbone buckling in rolled strip. J Eng Manuf 221: 143–150
23. ABAQUS Documentation. Reference document for ABAQUS/CAE, including ABAQUS/Viewer., Ver. 6.9
24. Altan T, Gegel HL (1983) Metal forming fundamental and application. ASM, Metal Park, OH 44073, Carner, Pub, Service, Inc, USA
25. Bland DR, Ford H (1948) The calculation of roll force and torque in cold strip rolling with tensions. Proc IME 159:144–153
26. Montmitonne P (2006) Hot and cold strip rolling processes. Comput Methods Appl Mech Eng 195:6604–6625
27. Dixon AE, Yuen WY (2008) A physical based method to predict spread and shape during flat rolling for real-time application. Steel Res Int 79:287–296
28. Cao J, Zhang J, Kong N, Mi K (2010) Finite element analysis of strip and rolling mills. Finite Element Analysis, Sciyo, Croatia, pp 561–588